The Hybrid Parametric Amplifier

COLIN S. AITCHISON AND A. WONG

Abstract—**This paper calculates the gain and noise performance of a new version of the parametric amplifier in which the signal circuit is part of an artificial transmission line while the idler circuit is resonant. A particularly useful property of this type of parametric amplifier is absence of oscillation with increasing pump power.**

I. Introduction

TWO VARIETIES of varactor parametric amplifiers have been proposed and examined in the past. The first of these is the resonant amplifier in which both the signal and idling circuits are resonant. The second is the traveling wave amplifier in which an artificial transmission line propagates the signal and idling frequencies, as well as the pump frequency [1]–[3].

In the resonant amplifier it is necessary to satisfy the constraint that

$$f_p = f_s + f_I$$

where

f_p the pump frequency
f_s the signal frequency
f_I the idling frequency.

In the traveling wave amplifier an additional constraint has to be satisfied at each varactor: this is a phase constraint and arises from the fact that the signal, idling, and pump signals must have the relationship

$$\theta_p = \theta_s + \theta_I$$

where p, s, and I refer to the pump, signal, and idling frequencies, respectively, and θ is the phase.

In the past alot of work was devoted to the traveling wave amplifier because of its attractive bandwidth potential, but it proved difficult to satisfy this phase relationship over a large bandwidth when an artificial transmission loaded with lumped varactors was used [4].

This paper proposes and examines the properties of a combination of the resonant and traveling wave parametric amplifier. The name *hybrid parametric amplifier* is used for this combination [5].

II. The Hybrid Parametric Amplifier

The objective of the hybrid parametric amplifier is to avoid the phase constraint of the traveling wave amplifier by arranging that the idling circuit associated with each varactor is resonant while retaining the traveling wave signal circuit. It is assumed that the pump power is fed to each varactor separately, though this is not essential.

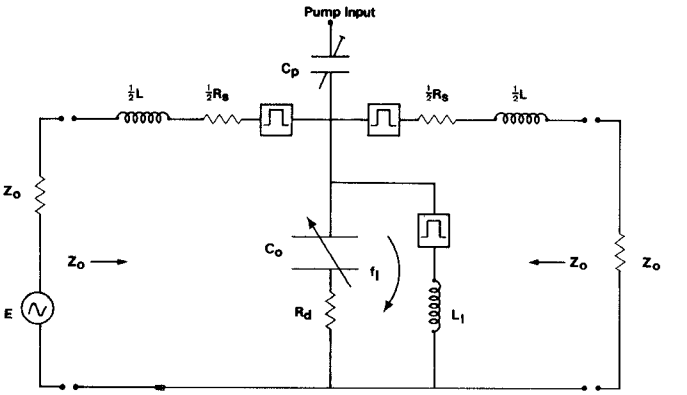

Fig. 1. Single T section of hybrid parametric amplifier.

It will be shown that the hybrid amplifier has a number of additional advantages. These are stated as follows.

a) The amplifier cannot oscillate.
b) The variation of gain with pump power has a zero minimum at which value the gain is the designed maximum value.
c) Since the signal circuit is not resonant, the loss associated with the signal circuit inductance can be less than in a conventional resonant parametric amplifier. This is of importance at low frequencies (such as IF frequencies) since at these frequencies the resonant parametric amplifier noise figure is seriously degraded due to the loss associated with this inductance [ ].

Fig. 1 shows a single T section of artificial transmission line (at the signal frequency) of characteristic impedance Z_0, which is fed from a generator E of internal impedance Z_0 and is terminated in a load Z_0. Both series elements consist of inductances $1/2L$, with series loss $1/2R_s$. The shunt element is a varactor of capacitance C_0 and series resistance R_d. In shunt with the varactor is an inductance L_I which resonates the varactor at the idling frequency. Bandpass filters are provided in both series arms and in series with the idling inductance so that signal and idling currents flow only in the appropriate circuits. Pump power is fed to the midpoint of the T section through a series capacitor.

Fig. 2 shows the arrangement of three cascaded T sections with separate pump feeds. The signal circuit series inductance L has a shunt capacitance placed across it, forming a parallel resonant circuit at the idling

Manuscript received August 24, 1979; revised March 19, 1980.
C. S. Aitchison is with the Electronics Department, Chelsea College, Pulton Place, London SW6 5PR, England.
A. Wong was with the Electronics Department, Chelsea College, Pulton Place, London SW6 5PR, England.

0018-9480/80/0800-0833$00.75 ©1980 IEEE

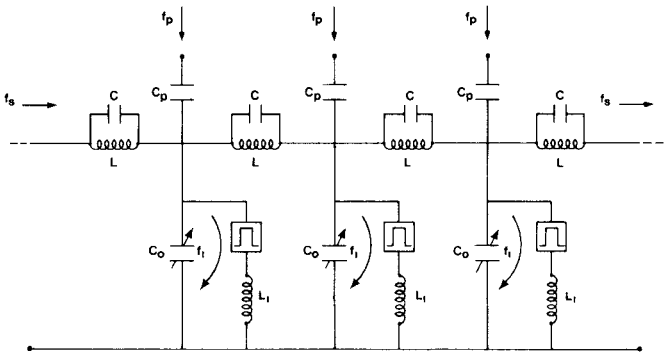

Fig. 2. Three cascaded hybrid parametric amplifier T sections.

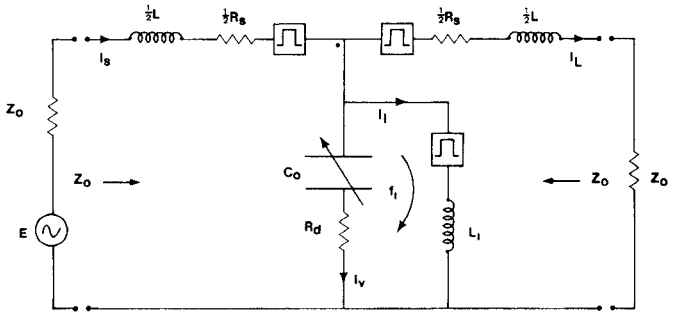

Fig. 3. Single stage hybrid parametric amplifier showing circuit parameters.

frequency, serving as a filter to constrain idling energy to the appropriate idling circuit in each section.

$$C=\frac{C_0}{\left[1+\gamma(\exp j\omega_p t+\exp -j\omega_p t)\right]}$$

where $0>\gamma>0.5$.

Applying Kirchhoff's Laws to the signal circuit we get

$$e=\left(Z_0+\tfrac{1}{2}Z_s\right)i_s+\left(R_d-\frac{j}{C_0\omega_s}\right)i_v-\frac{j\gamma i_I^*}{C_0\omega_I} \tag{1}$$

$$e=\left(Z_0+\tfrac{1}{2}Z_s\right)i_s+\left(Z_0+\tfrac{1}{2}Z_s\right)i_L \tag{2}$$

$$i_s=i_v+i_L. \tag{3}$$

In (1), (2), and (3) we have used the complex notation for current and voltage.

For the idler circuit (using resonant parametric amplifier theory [1]) we have

$$0=i_I(r_I+j\omega_I L_I)-\frac{ji_I}{C_0\omega_I}-\frac{j\gamma i_v^*}{C_0\omega_s}. \tag{4}$$

If we resonate the idler circuit (4) simplifies to

$$i_I=\frac{j\gamma i_v^*}{C_0\omega_s r_I}. \tag{5}$$

Substituting the starred version of (5) into (1) and (3) gives

$$e=\left(Z_0+\tfrac{1}{2}Z_s\right)i_s+\left(R_d-\frac{j}{C_0\omega_s}-\frac{\gamma^2}{C_0^2\omega_s\omega_I r_I}\right)i_v. \tag{6}$$

To obtain an expression for gain we need to know i_L in terms of e. Substituting (6) into (2) and (3) gives

$$i_L=\frac{\left(R_d-\frac{j}{C_0\omega_s}-\frac{\gamma^2}{C_0^2\omega_s\omega_I r_I}\right)e}{\left[Z_0+\frac{1}{2}(R_s+j\omega_s L)\right]\left[Z_0+\frac{1}{2}(R_s+j\omega_s L)+2\left(R_d-\frac{j}{C_0\omega_s}-\frac{\gamma^2}{C_0^2\omega_s\omega_I r_I}\right)\right]} \tag{7}$$

or

$$|I_L|^2=\frac{\left[(R_d-R_n)^2+\frac{1}{\omega_s^2C_0^2}\right]|E|^2}{\left[\left(Z_0+\frac{1}{2}R_s\right)^2+\left(\frac{\omega_s L}{2}\right)^2\right]\left[\left(Z_0+\frac{1}{2}R_s+2R_d-2R_n\right)^2+\left(\frac{4}{\omega_s^2C_0^2}\right)\left(1-\frac{\omega_s^2LC_0}{4}\right)^2\right]} \tag{8}$$

III. Gain Performance of the Hybrid Parametric Amplifier

We wish to examine the dependance of the available gain of a single T section on the T-section circuit parameters.

The circuit we wish to analyze is shown in Fig. 3. The current in the first series arm is I_s and in the second arm is I_L. The current flowing through the varactor is I_v and that flowing in the idling circuit is I_I.

We assume the capacitance C_0 to be pumped at a frequency ω_p where ω_p is equal to sum of the signal frequency ω_s and the idler frequency ω_I. We write the instantaneous value of the pumped capacitance as

where

$$R_n=\frac{\gamma^2}{C_0^2\omega_s\omega_I r_I}.$$

This expression (8) simplifies if we assume a value of R_n which makes the term $(Z_0+\frac{1}{2}R_s+2R_d-2R_n)$ in the denominator vanish, i.e.,

$$\left(Z_0+\tfrac{1}{2}R_s+2R_d-2R_n\right)=0. \tag{9}$$

We now calculate the dependance of the available gain corresponding to this condition and write this as $G_{\text{av,max}}$ where G_{av} is given by

$$G_{\text{av}}=\frac{i_L i_L^* Z_0}{ee^*/(4Z_0)}. \tag{10}$$

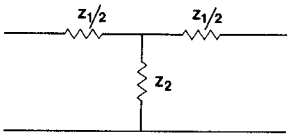

Fig. 4. General T section.

We obtain, if $1/2R_s \ll Z_0$

$$G_{\text{av,max}} = \frac{\left[1+\left(\frac{\omega_s C_0 Z_0}{2}\right)^2\right]}{\left[1+\left(\frac{\omega_s L}{2Z_0}\right)^2\right]\left[1-\frac{\omega_s^2 LC_0}{4}\right]^2}. \quad (11)$$

We now need an expression for Z_0. For the T section shown in Fig. 4, with two series arms each of impedance $1/2Z_1$ and a shunt arm impedance of Z_2 it can be shown that

$$Z_0 = \sqrt{Z_1 Z_2\left(1+\tfrac{1}{4}\frac{Z_1}{Z_2}\right)}. \quad (12)$$

If the loss (or gain) terms associated with the complex impedances in (12) are small in comparison to the reactive terms this can be simplified to

$$Z_0 = \sqrt{\frac{L}{C_0}\left(1-\frac{\omega_s^2 LC_0}{4}\right)}. \quad (13)$$

Substitution of (13) into (11) gives

$$G_{\text{av,max}} = \frac{\left[1+\frac{\omega_s^2 LC_0}{4}\left(1-\frac{\omega_s^2 LC_0}{4}\right)\right]}{\left[1+\frac{\omega_s^2 LC_0}{4}\Big/\left(1-\frac{\omega_s^2 LC_0}{4}\right)\right]\left[1-\frac{\omega_s^2 LC_0}{4}\right]^2}. \quad (14)$$

In (14) the term $\omega_s^2 LC_0/4$ is significant and we give it the symbol g, i.e.,

$$g = \frac{\omega_s^2 LC_0}{4}. \quad (15)$$

We see from (13) that g must be less than unity so that Z_0 is real and a signal can propagate through the T section. Physically g is the square of the ratio of signal frequency to cutoff frequency (f_c) of the artificial transmission line, i.e.,

$$g = \left(\frac{f_s}{f_c}\right)^2. \quad (16)$$

The cutoff frequency of the artificial transmission line is defined by

$$f_c = \frac{1}{\pi\sqrt{LC_0}}. \quad (17)$$

We can write (14) in terms of g as

$$G_{\text{av,max}} = \frac{1+g(1-g)}{\left(1+\frac{g}{1-g}\right)(1-g)^2}. \quad (18)$$

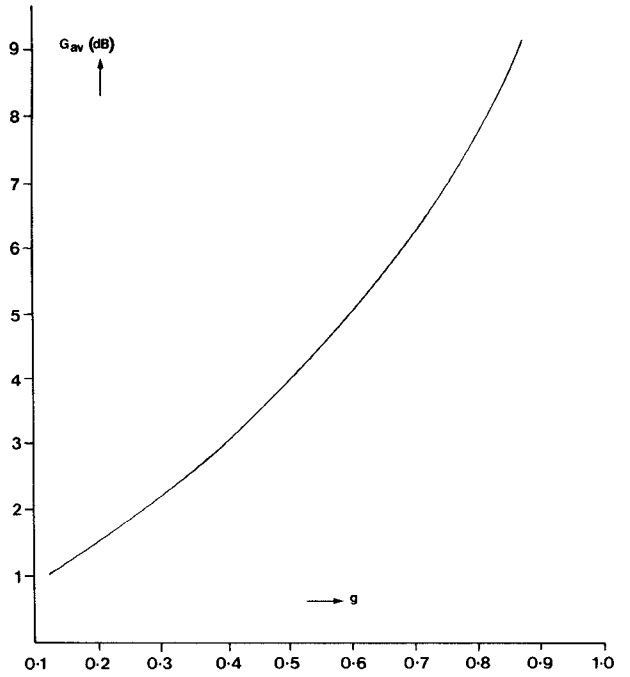

Fig. 5. Dependence of available gain on g.

This simplifies to

$$G_{\text{av,max}} = g + \frac{1}{(1-g)}. \quad (19)$$

The variation of $10\log_{10} G_{\text{av,max}}$ with the parameter g is shown in Fig. 5, showing that useful gain is obtainable for moderate values of g.

We previously used R_n for the terms $\gamma^2/(C_0^2\omega_s\omega_I r_I)$. Since, in practice, the idling loss r_I is due to the varactor alone, we can write R_n as

$$R_n = \frac{\gamma^2}{C_0^2\omega_s\omega_I R_d}. \quad (20)$$

By substituting (9) in (20) we connect ω_I with Z_0; thus

$$1 = \frac{\gamma^2}{C_0^2\omega_S\omega_I R_d\left(\frac{1}{2}Z_0+\frac{1}{4}R_s+R_d\right)}. \quad (21)$$

The selection of the parameters of a hybrid parametric amplifier proceeds in the following sequence.

a) For a given varactor (specifying C_0, γ, and R_d) select L so that the required stage gain is achieved at the specified signal frequency using (18) and (15).
b) Use (13) to determine Z_0.
c) Use (21) to determine ω_I.

If the calculated values of Z_0 or ω_I are practically inconvenient, they can be changed by selection of a different varactor.

Examination of (8) shows that the current through the load is determined by the value of R_n in the second term in the denominator. (The effect of the R_n term in the numerator is small since $|R_n| \gg R_d$ and this term can be neglected.) As γ increases from zero the available gain increases to its maximum value (at the optimum γ) and then reduces with further increase of γ. A plot of

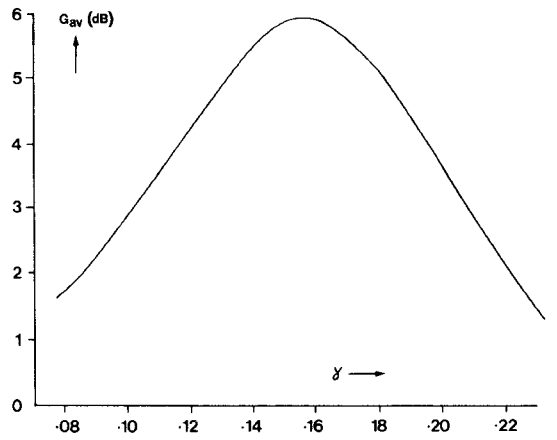

Fig. 6. Theoretical variation of gain as a function of γ.

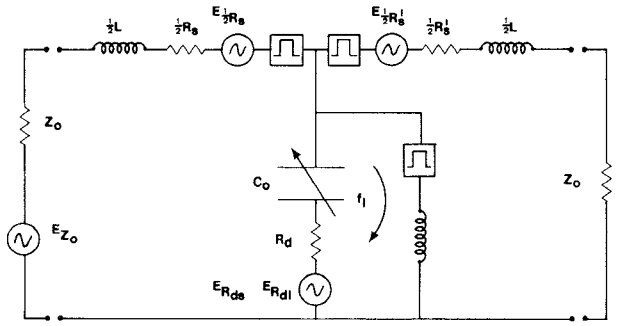

Fig. 7. Noise equivalent circuit for the hybrid paramp.

$10 \log_{10} G_{av}$ against γ shows the symmetry of thin curve, and an example of such a curve is shown in Fig. 6, showing a maximum stage gain of 6 dB at an optimum $\gamma(\gamma_{opt})$ of 0.15. This feature of the hybrid parametric amplifier is a significant advantage over the conventional resonant parametric amplifier, and removes the need for a stable pump source.

IV. The Noise Figure of the Parametric Hybrid Amplifier

We wish to calculate the noise figure of the hybrid parametric amplifier.

We first calculate the noise figure of the single T section (of characteristic impedance Z_0 terminated and fed from Z_0) shown in Fig. 7.

The noise sources dissipating power in the load of the amplifier are the following:

1) the source resistance Z_0 at the standard temperature T_0 in the signal circuit;

2) the series losses ($1/2R_s$ and $1/2R_s'$) in the signal circuit (R_s and R_s' are identical but are separated symbolically since the power dissipated in the load is different in the two cases);

3) the varactor loss R_d in the signal circuit;

4) the varactor loss R_d in the idler circuit which produces noise in the signal circuit by frequency conversion.

We assume that shot, flicker, and pump noise are negligible in comparison with thermal noise and, for simplicity, that the amplifier is operating at the standard temperature (290 K) as specified in the noise figure definition [5].

The noise power dissipated in the load Z_0 due to the source (E_{Z_0}) is obtained from (8).

With the optimum condition given by (9) the current through the load I_L is then

$$I_L^2 = \frac{E_{Z_0}^2\left[\frac{1}{4}\left(Z_0+\frac{1}{2}R_s\right)^2+\left(\frac{1}{\omega_s C_0}\right)^2\right]}{\left[\left(Z_0+\frac{1}{2}R_s\right)^2+\left(\frac{\omega_s L}{2}\right)^2\right]\left[\left(\frac{2}{\omega_s C_0}\right)^2\left(1-\frac{\omega_s^2 L C_0}{4}\right)^2\right]} \tag{22}$$

where $E_{Z_0}^2$ is equal to $4kT_0Z_0B$, and Z_0 is assumed to be real.

Neglecting $1/2R_s$ in comparison with Z_0 and substituting g for $\omega_s^2 LC_0/4$ we get

$$I_L^2 = \frac{E_{Z_0}^2\left[1+g(1-g)\right]}{4Z_0^2\left[1+\frac{g}{1-g}\right](1-g)^2}. \tag{23}$$

The noise power dissipated in the load Z_0, written $P_{Z_0}(Z_0)$, is given by

$$P_{Z_0}(Z_0) = kT_0B\left(g+\frac{1}{1-g}\right). \tag{24}$$

The noise power dissipated in the load Z_0 due to the inductance loss $1/2R_s$ is $I_L^2 Z_0$ where I_L is given by

$$I_L^2 = \frac{E_{\frac{1}{2}R_s^2}\left[\frac{1}{4}\left(Z_0+\frac{1}{2}R_s\right)^2+\left(\frac{1}{\omega_s C_0}\right)^2\right]}{\left[\left(Z_0+\frac{1}{2}R_s\right)^2+\left(\frac{\omega_s L}{2}\right)^2\right]\left[\left(\frac{2}{\omega_s C_0}\right)^2\left(1-\frac{\omega_s^2 L C_0}{4}\right)^2\right]} \tag{25}$$

$$E_{1/2R_s}^2 = 4kT_0\left(\tfrac{1}{2}R_s\right)B.$$

Neglecting $1/2R_s$ in comparison with Z_0 in (25) we get

$$I_L^2 = \frac{E_{1/2R_s}^2\left(g+\frac{1}{1-g}\right)}{4Z_0^2} \tag{26}$$

so that the power dissipated in the load $P_{1/2R_s}(Z_0)$ is

$$P_{1/2R_s}(Z_0) = \frac{kT_0B}{q}\left(g+\frac{1}{1-g}\right) \tag{27}$$

where $Z_0/1/2R_s$ is written as q.

In order to calculate the noise power dissipated in the load Z_0 from the second inductance loss ($1/2R_s'$), we need to calculate the current I_L, in the load due to a generator $e_{1/2R_s'}$, in series with the second inductance in the T section as shown in Fig. 8.

Applying Kirchhoff's Laws to this circuit we have

$$e_{1/2R_s'} = i_L Z_1 + i_v\left(R_d - \frac{j}{C_0\omega_s}\right) - j\frac{i_I^*\gamma}{C_0\omega_I} \tag{28}$$

$$i_L = i_v + i_s \tag{29}$$

$$e_{1/2R_s'} = i_L Z_1 + i_s Z_1 \tag{30}$$

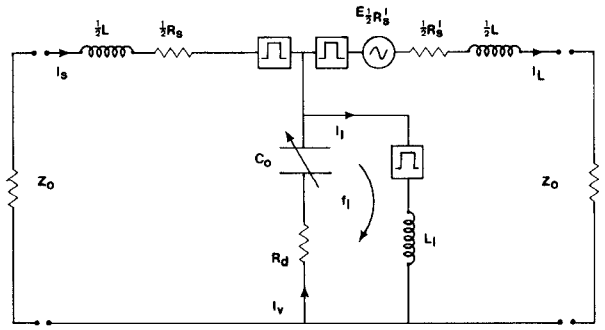

Fig. 8. T section with noise from $1/2R_s'$.

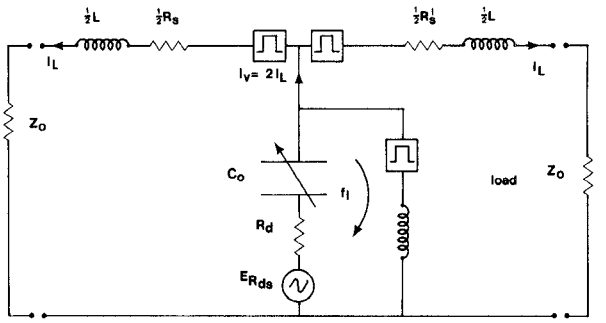

Fig. 9. T section with noise from R_d.

where

$$Z_1 = Z_0 + \tfrac{1}{2}Z_s$$

$$Z_s = R_s + j\omega_s L.$$

From (5) we get

$$i_I^* = \frac{-ji_v\gamma}{C_0\omega_s r_I}. \tag{31}$$

Equations (28) and (31) give

$$e_{1/2R_s'} = i_L Z_1 + (i_L - i_s)\left[Z_2 - \frac{\gamma^2}{C_0^2\omega_s\omega_I R_I} \right] \tag{32}$$

where

$$Z_2 = R_d - \frac{j}{C_0\omega_s}.$$

Substituting (30) into (32) gives

$$e_{1/2R_s'} = i_L Z_1 + \left(i_L - \frac{e_{1/2R_s'} - i_L Z_1}{Z_1} \right)(Z_2 - R_n). \tag{33}$$

Starring (33) and multiplying by (33) gives

$$I_L^2 = \frac{E_{1/2R_s}^2\left[\left(Z_0 + \tfrac{1}{2}R_s + R_d - R_n\right)^2 + \left(\frac{\omega_s L}{2} - \frac{1}{\omega_s C_0}\right)^2 \right]}{\left[\left(Z_0 + \tfrac{1}{2}R_s\right)^2 + \left(\frac{\omega_s L}{2}\right)^2 \right]\left[\left(Z_0 + \tfrac{1}{2}R_s + 2R_d - 2R_n\right)^2 + \left(\frac{\omega_s L}{2} - \frac{2}{C_0\omega_s}\right)^2 \right]}. \tag{34}$$

The maximum current occurs when

$$\left(Z_0 + \tfrac{1}{2}R_s + 2R_d - 2R_n\right) = 0$$

in accordance with (9). Equation (34) then simplifies to

$$I_L^2 = \frac{E_{1/2R_s'}^2}{4Z_0^2}\left[g + \frac{(1-2g)^2}{(1-g)} \right] \tag{35}$$

and the noise power $P_{1/2R_s'}(Z_0)$, dissipated in the load Z_0, due to $e_{1/2R_s'}$ is given by

$$P_{1/2R_s'}(Z_0) = \frac{kT_0B}{q}\left[g + \frac{(1-2g)^2}{(1-g)} \right]. \tag{36}$$

The noise power dissipated in the load Z_0, due to the varactor loss R_d, at the signal frequency can be calculated by placing a generator $R_{R_{ds}}$ in series with the varactor as shown in Fig. 9.

Applying Kirchhoff's Laws to this circuit we have

$$e_{R_{ds}} + i_v\left(R_d - \frac{j}{C_0\omega_s} \right) - \frac{ji_I^*\gamma}{C_0\omega_I} + i_L Z_1 = 0 \tag{37}$$

$$i_v = 2i_L \tag{38}$$

where

$$Z_1 = Z_0 + \tfrac{1}{2}R_s + \frac{j\omega_s L}{2}.$$

Using (31) in (37) and eliminating i_v using (38) we get

$$i_L = \frac{-e_{R_{ds}}}{\left(Z_0 + \tfrac{1}{2}R_s + 2R_d - 2R_n\right) + j\left(\frac{\omega_s L}{2} - \frac{2}{C_0\omega_s}\right)}. \tag{39}$$

Starring (39) and multiplying gives

$$I_L^2 = \frac{E_{R_{ds}}^2}{\left(\frac{2}{C_0\omega_s}\right)^2\left(1 - \frac{\omega_s^2 LC_0}{4}\right)^2}. \tag{40}$$

But

$$E_{R_{ds}}^2 = 4kT_0R_dB$$

so that the power dissipated in the load Z_0 due to the generator $E_{R_{ds}}$ is given by

$$P_{R_{ds}}(Z_0) = \frac{kT_0B}{p}\left(\frac{2g}{1-g}\right) \tag{41}$$

where p is equal to $Z_0/2R_d$.

The varactor loss R_d also gives an idling frequency current in the idler circuit which gives rise to a current at the signal frequency in the load Z_0.

The generator $E_{R_{dI}}$ is shown in the idler circuit in Fig. 10.

Applying Kirchhoff's Laws

$$0 = 2i_L\left(R_d - \frac{j}{C_0\omega_s} \right) - \frac{ji_I^*\gamma}{C_0\omega_I} + i_L Z_1 \tag{42}$$

$$e_{R_{dI}} = i_I r_I - \frac{2j\gamma i_L^*}{C_0\omega_s} \tag{43}$$

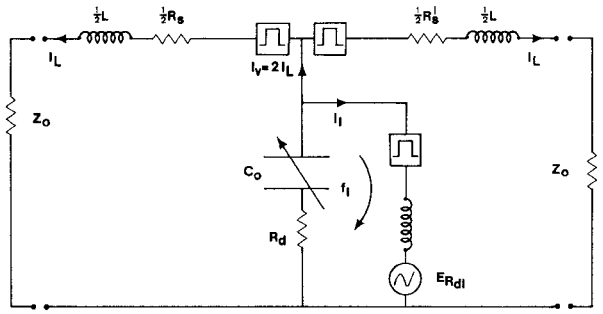

Fig. 10. T section with noise at the idler frequency from R_d.

where we have assumed the idler circuit to be resonant.

Substituting (43) into (42) gives an expression for i_L

$$i_L = \frac{\frac{j\gamma}{C_0\omega_I r_I} e^*_{R_{dI}}}{\left[Z_0 + \frac{1}{2}R_s + 2R_d - 2R_n + j\left(\frac{\omega L}{2} - \frac{2}{\omega C_0}\right)\right]} \tag{44}$$

giving

$$|I_L|^2 = \frac{\left(\frac{\gamma}{C_0\omega_I r_I}\right)^2 |E_{R_{dI}}|^2}{\left(Z_0 + \frac{1}{2}R_s + 2R_d - 2R_n\right)^2 + \left(\frac{\omega_s L}{2} - \frac{2}{\omega_s C_0}\right)^2}. \tag{45}$$

As before we put

$$Z_0 + \tfrac{1}{2}R_s + 2R_d - 2R_n = 0 \tag{46}$$

$$r_I = R_{dI}. \tag{47}$$

We know that R_n is given by

$$R_n = \frac{\gamma^2}{C_0^2\omega_s\omega_I R_d}. \tag{48}$$

Substituting (46) and (47) in (48) gives

$$\left(\frac{\gamma}{C_0\omega_I r_I}\right)^2 = \frac{f_s}{f_I}\left(1 + p + \frac{p}{q}\right). \tag{49}$$

Substituting (49) into (45) gives for the power dissipated in Z_0 due to the generator $E_{R_{dI}}(P_{R_{dI}}(Z_0))$ the relation

$$P_{R_{dI}}(Z_0) = \frac{4kT_0R_dBZ_0}{\left(\frac{2}{\omega_s C_0}\right)^2\left(1 - \frac{\omega_s^2 LC_0}{4}\right)^2}\frac{f_s}{f_I}\left(1 + p + \frac{p}{q}\right). \tag{50}$$

But

$$E^2_{R_{dI}} = 4kT_0R_dB. \tag{51}$$

Substituting (51) into (50) and expressing in terms of g we get

$$P_{R_{dI}}(Z_0) = \frac{kT_0B}{p}\left(\frac{2g}{1-g}\right)\left(1 + p + \frac{p}{q}\right)\frac{f_s}{f_I}. \tag{52}$$

We can now calculate the noise figure F_1 of one stage using the standard definition [5].

$$F_1 = \frac{P_{Z_0}(Z_0) + P_{1/2R_s}(Z_0) + P_{1/2R_s}(Z_0) + P_{R_{dI}}(Z_0) + P_{R_{dI}}(Z_0)}{P_{Z_0}(Z_0)}. \tag{53}$$

Substituting using (24), (27), (36), (41), and (52) gives on rearranging

$$F_1 = 1 + \frac{2}{q}\left[\frac{1-g(1-g)}{1+g(1-g)}\right] + \frac{2g}{1+g(1-g)}\left[\frac{1}{p} + \frac{f_s}{f_I}\left(1 + \frac{1}{p} + \frac{1}{q}\right)\right]. \tag{54}$$

The gain of a single stage hybrid amplifier is likely to be low and, therefore, it is more useful to calculate the noise measure M [6], [7]. This is given by the relationship

$$M = \frac{F_1 - 1}{1 - \frac{1}{G_{av}}} \tag{55}$$

and is the excess noise figure of an infinite number of cascaded stages each of noise figure F_1 and available gain G_{av}.

Using (19) and (55) M is given by

$$M = \frac{2}{q}\left[\frac{1-g(1-g)}{g(2-g)}\right] + \frac{2}{(2-g)}\left[\frac{1}{p} + \frac{f_s}{f_I}\left(1 + \frac{1}{p} + \frac{1}{q}\right)\right]. \tag{56}$$

Both (54) and (56) degenerate to form conventional resonant parametric amplifier noise expressions if there is no loss associated with the signal circuit inductance, since q is then infinite.

V. Advantages of the Hybrid Parametric Amplifier

The gain and noise figure theory for the hybrid parametric amplifier detailed in the preceding paragraphs shows that the current in the signal circuit cannot rise to infinity and hence the amplifier cannot oscillate. This is a significant advantage of the hybrid parametric amplifier.

The expressions for noise figure include a thermal noise contribution from the loss associated with the inductors of the series arms of the T section. Since these inductors are smaller than the corresponding inductance used in a corresponding resonant parametric amplifier with the same varactor, we may expect the noise performance of the hybrid parametric amplifier to be superior at these frequencies at which the loss in the inductance is not negligible compared with that in the varactor. Thus a hybrid parametric amplifier at 30 MHz should give a significantly better noise performance than that of the resonant version at frequencies below 100 MHz.

A companion paper [8] details the design construction and evaluation of a hybrid parametric amplifier at 30 MHz pumped in the UHF band with a 6-dB gain, 8-MHz bandwidth, and 18 K noise temperature.

VI. Conclusions

The concept of the hybrid parametric amplifier has been introduced and the gain and noise figure of a single T section have been calculated in terms of the varactor parameters and signal circuit inductance properties. The noise figure has been extended, in terms of noise measure,

to cover the behavior of n identical cascaded stages.

Gain dependence on pump power and low frequency (below UHF) noise behavior are expected to be attractive.

References

[1] L. A. Blackwell and K. L. Kotzebe, *Semiconductor Diode Parametric Amplifiers*. Englewood Cliffs, N. J.: Prentice-Hall, 1961.

[2] R. L. Honey, and E. M. T. Jones, "A wide-band UHF travelling wave variable reactance amplifier," *IRE Trans. Microwave Theory Tech*, vol. MTT-8, pp. 351–361, May 1960.

[3] C. V. Bell and G. Wade, "Circuit considerations in travelling-wave parametric amplifiers," *IRE WESCON Conv. Rec*, Pt. 2, pp. 75–82, 1959.

[4] R. S. Engelbrecht, "Non-linear-reactance (parametric) travelling-wave parametric amplifiers for UHF," *Dig. Tech. Papers*, 1959 Solid State Circuit Conf., Philadelphia, PA, Feb. 12, 1959.

[5] "Standards on Receivers, definition of terms 1952," *Proc. IRE*, vol. 40, p. 1681, 1952.

[6] H. A. Haus and R. B. Adler, "Optimum noise performance of linear amplifiers," *Proc. IRE*, vol. 46, pp. 1517–1533, Aug. 1958.

[7] ——, *Circuit theory of Linear Noisy Networks*. New York: Technology and Wiley, 1959.

[8] C. S. Aitchison and A. Wong, "A VHF hybrid parametric amplifier," this issue, pp. 825–832.

High-Accuracy WKB Analyses of α-Power Graded-Core Fibers

KIMIYUKI OYAMADA, STUDENT MEMBER, IEEE, AND TAKANORI OKOSHI, MEMBER, IEEE

Abstract—**The WKB method is an effective approach to the analyses of propagation characteristics of optical fibers. However, conventional WKB analyses can not be applied to close-to-cutoff modes because the effect of core-cladding boundary is not considered exactly.**

This paper proposes two improved WKB analyses which consider the above effect more exactly. Both of these methods are applicable to the close-to-cutoff modes. The first one is superior in accuracy (for example, relative error in cutoff frequencies $\lesssim 10^{-5}$), but applicable only to quadratic profiles. The second one is applicable to general α-power profiles; the accuracy is poorer but tolerable for most practical purposes.

I. Introduction

MANY METHODS have been developed for the analysis of propagation characteristics of optical fibers having arbitrary refractive-index profiles. Among these, the WKB method [1],[2] is relatively simple and comprehensive. However, it is essentially an approximate analysis, and usually gives large error for close-to-cutoff modes.

A significant fact found by the conventional WKB analyses was that the multimode dispersion was minimized for a quasiquadratic (parabolic) profile [1]. It was also found that the maximum delay difference between propagating modes for such a profile was approximately $T\Delta^2/2$, where T and Δ denote the propagation time and the relative refractive-index difference (see (1)), respectively.

However, more exact analyses such as those by Rayleigh–Ritz method [3], finite-element method [4], and power-series expansion method [5] reveal that the delay-time difference between the well-confined and close-to-cutoff modes approaches $T\Delta$. This value is much greater than the above WKB prediction: $T\Delta^2/2$. The principal reason for such an error in the conventional WKB analyses [1],[2] is that the effect of the discontinuity in the slope of the index profile at core-cladding boundary is not taken into account. For the same reason, the effect of the index valley at the core-cladding boundary, which is claimed to be effective for reducing the multimode dispersion [6], cannot be analyzed by the conventional WKB analyses. Recently, Olshansky [7] and Ikuno [8] proposed modified WKB analyses to improve these drawbacks.

This paper proposes two WKB analyses which consider the above effect more exactly. These are applicable either to the close-to-cutoff modes or to the index profiles with valley. The first method is somewhat similar to the Olshansky's, but the accuracy is improved. The relative error in the cutoff frequencies of LP_{ml} modes in quadratic-profile fibers is below 10^{-5} for most modes. However, this method is difficult to apply to index profiles other than the quadratic one. The second method uses an asymptotic solution different from the first, and is applicable to general α-power profiles; however, the accuracy is poorer.

II. WKB Formulations

The index profile is assumed to be expressed as

$$n(r) = n_1\left[1 - 2\Delta f(r)\right]^{1/2} \tag{1}$$

where r denotes the radial coordinate normalized by the core radius a, and $f(r)$ is a function given as

$$f(r) = \begin{cases} r^\alpha, & r \leqslant 1 \quad (2) \\ 1, & r > 1. \quad (3) \end{cases}$$

In this case, the scalar wave equation [9] can be written as

$$\frac{1}{r}\frac{d}{dr}\left(r\frac{dR}{dr}\right) + \left\{u^2 - v^2 f(r) - \frac{m^2}{r^2}\right\} R = 0 \tag{4}$$

where $R(r)$ is the function representing the field distribution

Manuscript received January 7, 1980; revised March 18, 1980.

The authors are with the Department of Electrical Engineering, University of Tokyo, Bunkyo-ku, Tokyo 113, Japan.

0018-9480/80/0800-00839$00.75 ©1980 IEEE